# Synthesis and study of gold nanoparticles stabilized by bioflavonoids

*L. A. Levchenko, S. A. Golovanova, N. V. Lariontseva, A. P. Sadkov, D. N. Voilov, Yu. M. Shul´ga, N. G. Nikitenko, and A. F. Shestakov**

*Institute of Problems of Chemical Physics of the Russian Academy of Sciences, 1 prosp. Akad. Semenova, 142432 Chernogolovka, Moscow Region, Russian Federation. Fax: +7 (496) 522 3507. E-mail: a.s@icp.ac.ru; lidal@icp.ac.ru*

A new procedure for the preparation of biocompatible gold nanoparticles using bioflavonoids: rutin, quercetin, and luteolin as reducing agents and stabilizers was proposed. On varying the bioflavonoid concentration, nanoparticles of different size are formed. By the combined use of spectroscopy and atomic force microscopy, the nanoparticle size was estimated (40—50 nm). Uniform and highly dispersed gold nanoparticles were obtained at Au : rutin ratios of 1 : 1, 2 : 1, and 4 : 1 and Au : quercetin ratios of 2 : 1 and 4 : 1. The nanoparticle yield remains almost constant as the Au : rutin ratio varies over a broad range from 1 : 1 to 12 : 1. It was suggested that complete reduction of $Au^{III}$ to $Au^0$ with a large excess of Au is accompanied by extensive oxidation of bioflavonoid involving an intermediate oxidant formed in the system due to the high oxidative capacity of $Au^{III}$. For elucidating the catalytic role of bioflavonoids in the formation of gold nanoparticles, quantum chemical modeling of the process was performed.

**Key words:** gold, bioflavonoids, nanoparticles, synthesis, rutin, quercetin, luteolin, stabilization.

Currently, the interest in the preparation and study of gold nanoparticles (NP) is increasing, as they possess unique physicochemical properties[1—3] and are suitable for various applictions ranging from catalysis, sensor devices, and biomarkers to photonics, optoelectronics,[4] and medicine.[5] Recent studies have shown that gold NP have unusual and often unexpected catalytic properties,[5,6] which are manifested, as a rule, for small nanoparticle sizes.[7—9] It cannot be ruled out that catalysts based on gold compounds would provide a solution to the practically important task of selective oxidation of hydrocarbons with a cheap and pure oxidant, air oxygen.[10] Certain progress has been already achieved along this line, in particular, oxidation of compounds with activated C—H bonds and cyclohexene on an Au/C catalyst in solutions at 80 °C,[11] oxidation of benzaldehyde[12] and the nicotinamine—adenine—reduced dinucleotide (NADH)[13] system on gold NP, and oxidation of methane on supported gold NP[14] at temperature of >130 °C were performed.

We established the activation of methane under mild conditions in the presence of dodecanethiol-stabilized gold NP,[15] resulting in H/D exchange of methane with $D_2$. In addition, it was found that in the gold—bioflavonoid (rutin or quercetin) biomimetic system, catalytic sites performing selective NADH-dependent air oxygen oxidation of methane and lower alkanes to alcohols at room temperature are formed.[16,17] The mechanism of this interesting process is far from being clear due to the low concentra-

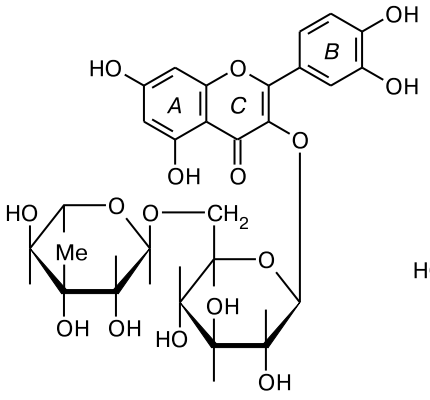


Rutin

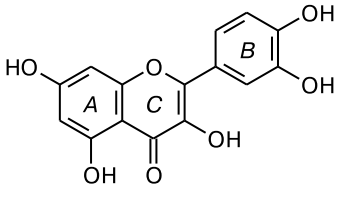


Quercetin

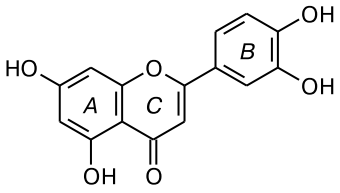


Luteolin

Published in Russian in *Izvestiya Akademii Nauk. Seriya Khimicheskaya,* No. 3, pp. 417—424, March, 2011.

tion of the active sites, which cannot be increased by a mere increase in the content of gold. A specific feature of the Au—bioflavonoid system is the formation of gold NP with time, as indicated by the appearance of a peak at 525—530 nm typical of gold NP in the absorption spectra. Therefore, the development of the method for targeted preparation of gold NP stabilized by bioflavonoids and study of their possible role in the alkane functionalization are topical issues.

Previously, gold NP have not been prepared using bioflavonoids. The design of quercetin-modified coatings on the Au surface aimed at the formation of highly sensitive copper ion-binding site[18] is the most closely related work in this respect. The promising direct approach to the one-stage synthesis of NP using various biocompatible reagents,[19—25] including amino acids,[26—28] is being actively developed. In this respect, it was also of interest to study the stabilizing action of bioflavonoids on gold NP in order to extend the range of available biocompatible gold NP that are used in medical diagnostics and therapy of cancer.[29]

This work is the first example of using bioflavonoids (rutin, quercetin, and luteolin) as the reducing agents and stabilizers in the preparation of gold NP. These compounds are polyphenols belonging to the group of vitamins P and having clear-cut chelating properties.[30—32]

## Experimental

Gold nanoparticles were prepared by reduction of chloroauric acid ($HAuCl_4 \cdot 4H_2O$) with bioflavonoids by a procedure similar to a previously proposed one.[33] A $10^{-2}$ *M* aqueous solution of $HAuCl_4$ (1.25 mL) was added dropwise with vigorous stirring over a period of 1—2 min to an aqueous solution of bioflavonoid (48.5 mL) with a specified concentration ($2.5 \cdot 10^{-4}$, $5 \cdot 10^{-4}$, $2 \cdot 10^{-3}$, $1.25 \cdot 10^{-4}$, $6.25 \cdot 10^{-5}$, $4.2 \cdot 10^{-5}$, or $2.1 \cdot 10^{-5}$ mol $L^{-1}$), and vigorous stirring was continued for an additional 15 min. The Au : bioflavonoid concentration ratio was 1 : 1, 1 : 2, 1 : 8, 2 : 1, 4 : 1, 6 : 1, and 12 : 1. The synthesis was carried out at 95—98 °C.

The visualization and study of the surface topology of the obtained gold NP were performed by atomic force microscopy. This was done using a NTEGRA Aura NT-MDT microscope (Zelenograd, Moscow Region) with a resolution of 3 Å. All measurements were carried out in the tapping mode using platinum-coated silicon conducting cantilevers. The radius of curvature was ~30 nm.

The absorption spectra were recorded on a Specord M-40 spectrometer. For rutin-stabilized gold NP (1 : 1), IR spectra were also recorded. For this purpose, a drop of the solution was placed on a paraffin substrate, dried, and examined using a Perkin—Elmer-spectrum-100 IR spectrometer. The nanoparticles were precipitated using a Heinz Janetzki centrifuge (Engelsdorf—Leipzig, 8000 rpm). The separated NP were washed with water for 10 min. Gold in the precipitate and in the supernatant was quantified by atomic absorption spectroscopy using an A.A.S.-3 Carl Ceiss Jena spectrometer. Commercial rutin, quercetin, luteolin, $HAuCl_4 \cdot 4H_2O$ (Sigma), sodium citrate (chemically pure grade), $KMnO_4$ (chemically pure grade), KI (chemically pure grade), and doubly distilled water were used.

## Results and Discussion

The Au—rutin NP were studied in most detail. The absorption spectra of the NP obtained at different Au : rutin ratios are presented in Fig. 1. According to experimental data, by varying the Au : bioflavonoid ratio, it is possible to obtain gold NP of different size. The stability of the obtained solutions and the NP size depend considerably on the bioflavonoid concentration. As can be seen from Fig. 1, upon an increase in the rutin concentration, the maximum of the NP plasmon absorption peak shifts to longer wavelengths from 530 to 580 nm. However, this shift is not uniform. When the Au : rutin ratios are 12 : 1, 4 : 1, 2 : 1, and 1 : 1 (see Fig. 1), the spectra have a clear-cut absorption maximum at 529.7, 530.6, 532.7, and 533.7 nm, respectively. The position of the maximum regularly shifts to longer wavelengths. According to published data,[34] this corresponds to an increase in the nanoparticle size from 43 to 51 nm. For Au : rutin ratios of 1 : 2 and 1 : 8 (see Fig. 1), the spectra are characterized by broad absorption with a maximum at ~570—580 nm, which attests to the presence of larger NP (~100 nm). The presence of the long-wavelength shoulder at ~700 nm and diffuse absorption at all wavelengths attest to a nonuniform composition of the NP caused apparently by their aggregation. Indeed, solutions of NP obtained with an excess of rutin with respect to gold are unstable and partly precipitate. Note a change in the color of the NP solution; upon an increase in the rutin concentration, the color changes from red to blue-violet. The absorption spectra of gold NP stabilized by quercetin and luteolin with the Au : bioflavonoid ratio of 1 : 1 differ little from the absorption spectra of gold NP with rutin (Fig. 2). According to the position of

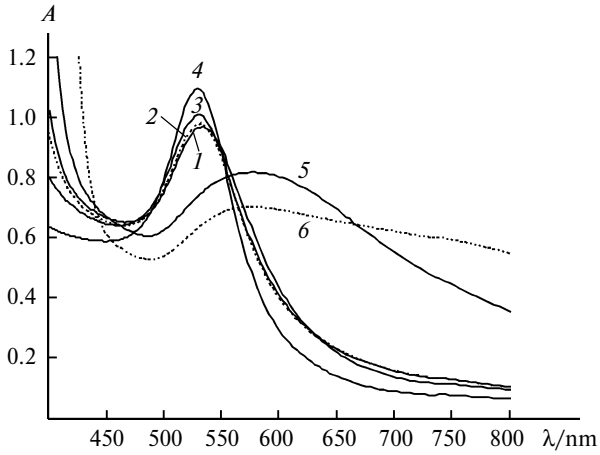


**Fig. 1.** Absorption spectra of rutin-stabilized gold NP at different Au : rutin ratios (10 mm cell): 1 : 1 (*1*), 2 : 1 (*2*), 4 : 1 (*3*), 12 : 1 (*4*), 1 : 2 (*5*), and 1 : 8 (*6*).

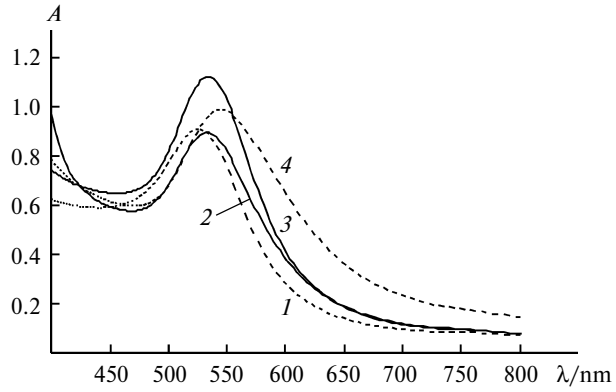


**Fig. 2.** Absorption spectra of gold NP stabilized by various compounds: (*1*) Na citrate (Zsigmondy sol), (*2*) rutin (1 : 1), (*3*) quercetin (1 : 1), (*4*) luteolin (1 : 1) (10 mm cell).

the absorption maximum, the Au—rutin and Au—quercetin NP have similar sizes, while the Au—luteolin NP are larger.

A distinctive feature of the Au—rutin NP obtained at 1 : 1, 2 : 1, and 4 : 1 ratios is the high temporal stability. As follows from the spectral data (Fig. 3), a slight decrease in the optical density without shift of the plasmon peak maximum occurs during the first month of storage of a solution of NP.

Atomic force microscopic images of rutin-, quercetin-, and luteolin-stabilized gold NP were obtained (Fig. 4). These data can be used for direct observation of the topography of gold NP and evaluation of their size uniformity. For the Au—rutin and Au—quercetin NP, the size distribution is more uniform and the predominating particle diameter, 40—50 nm, corresponds to the value calculated from spectral data. Conversely, Au—luteolin NP are less uniform in size (50—150 nm).

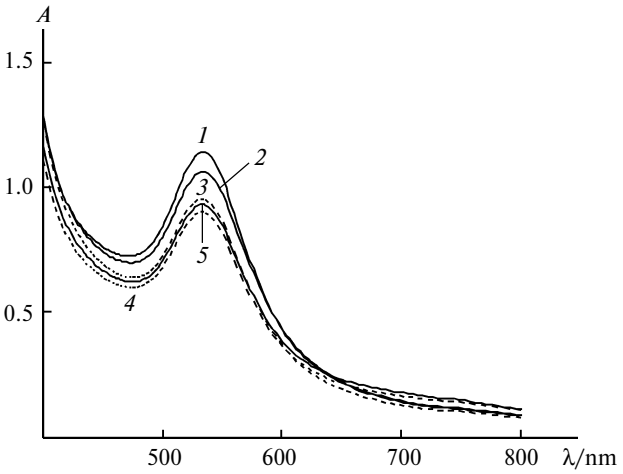


**Fig. 3.** Time variation of the absorption spectra of 1 : 1 rutin-stabilized gold NP (0 mm cell): (*1*) 1 h, (*2*) 2 days, (*3*) 1 month, (*4*) 6 months, (*5*) 9 months.

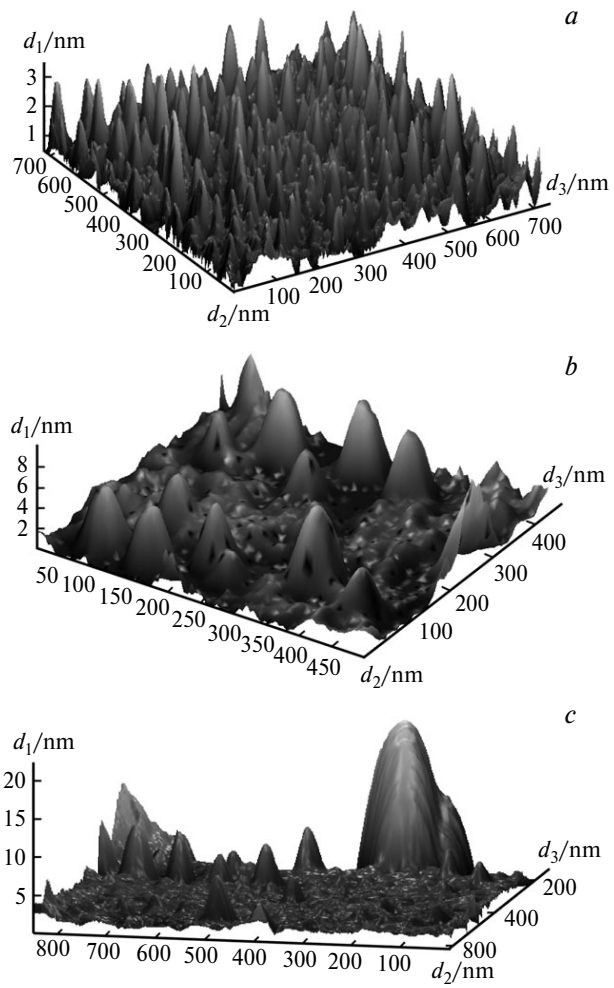


**Fig. 4.** Images of gold NP stabilized by rutin (*a*), quercetin (*b*), luteolin (*c*) deposited from an aqueous solution onto single-crystal silicon surface.

Figure 5 presents the IR spectra of paraffin-supported films, which were obtained by drying a colloid solution of gold NP at an Au : rutin ratio of 1 : 1 (curve *3*). For comparison, the IR spectra of the substrate (curve *1*), a film of an aqueous solution of rutin (curve *2*), and a film of washed NP (curve *4*) are shown in the same figure. The IR spectrum of NP (see Fig. *5*, curve *4*) shows four broad absorption peaks at 1065, 1375, 1649, and 3379 $cm^{-1}$. All of these, except for the peak at 1375 $cm^{-1}$, have analogs as one or several bands in the spectrum of rutin (curve *1*). Thus, the IR spectra of the Au—rutin NP bear some resemblance to the IR spectra of pure rutin, suggesting the presence of modified rutin molecules in the ligand shell of gold NP.

The IR spectrum of a solution of nanoparticles (see Fig. 5, curve *3*) reflects the characteristic features of both spectra (rutin and NP) and can be considered as some superposition thereof. This means that rutin occurs in two forms in a colloid solution of NP: in the ligand shell of the

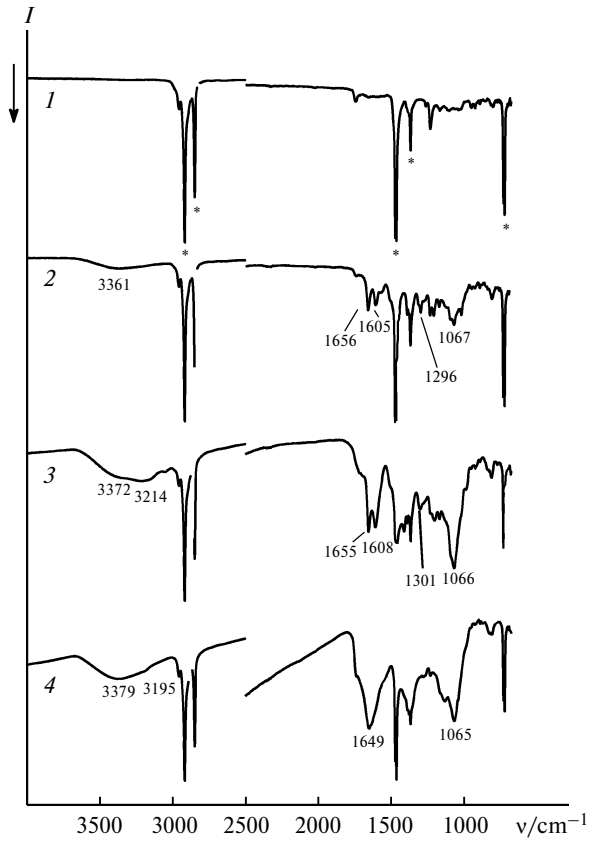


**Fig. 5.** IR spectra of the paraffin substrate (*1*), rutin (*2*), a solution of gold NP stabilized by rutin (*3*) and separated by centrifugation (*4*).

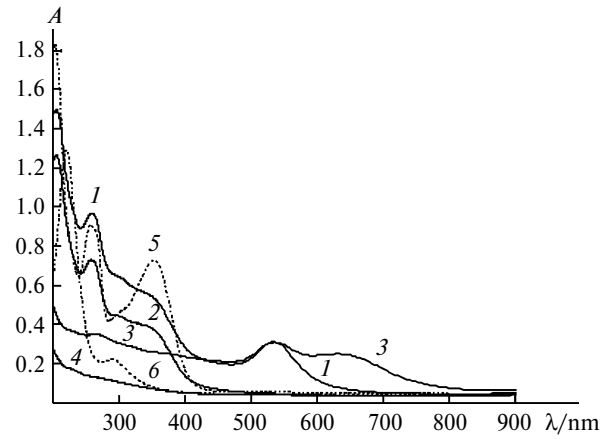


**Fig. 6.** Absorption spectra of Au—rutin NP before and after centrifugation (3 mm cell): (*1*) Au—rutin sol (1 : 1), (*2*) supernatant fraction of the Au—rutin sol (1 : 1), (*3*) precipitate of the Au—rutin sol (1 : 1), (*4*) supernatant fraction of the Au—rutin sol (6 : 1), (*5*) rutin, (*6*) $HAuCl_4$.

NP and in the dissolved state. The positions of individual peaks in curves *2* and *3* almost coincide. The greatest differences are observed in the peak intensity in the OH vibration region. For a solution of NP, this peak is more pronounced and an additional peak appears at 3214 $cm^{-1}$. This peak, although shifted to lower frequencies, also occurs in the NP spectrum as a shoulder at 3195 $cm^{-1}$.

According to chemical analysis data, in sols at Au : rutin = 1 : 1 and 6 : 1, most of gold (84 and 89%, respectively) occurs within the NP that precipitate upon centrifugation. The optical absorption spectra of the supernatant do not show the characteristic plasmon peak. This attests to almost complete precipitation of NP. During precipitation, partial coarsening of the particles takes place, as indicated by the shoulder at 650 nm in the optical spectrum of the precipitate (Fig. 6).

The presence of modified rutin within the NP implies its stabilizing function. The estimated fraction of surface atoms in ~40 nm sphere-like gold NP (<3%) provides the conclusion that a small portion of bioflavonoid (several percent relative to the gold content) can serve for stabilization of the gold NP.

Thus, from the set of obtained results, it follows that this procedure provides bioflavonoid-stabilized gold NP in high yield, these particles being apparently similar to those formed with time in the methane-oxidizing catalytic system. Preliminary experiments dealing with the catalytic properties of fractionated solutions of NP demonstrated that the supernatant fraction is much more active in the NADH oxidation than the precipitated fraction containing coarse gold NP. This activity is even an order of magnitude higher than the activity of previously studied Au—bioflavonoid systems.[16]

This result is of interest from the standpoint of analysis of active site structure. Since the supernatant fraction does not show a plasmon absorption peak, it can contain only soluble complexes or gold clusters. In other words, it is quite probable that the role of active sites in this system is played by some polynuclear Au complexes containing a bioflavonoid. Considering this hypothesis. one can at least understand why a 5-fold change in the gold content induces only a slight change in the methane oxidation properties.[16,17] This fact provides conclusion concerning the mechanism of formation of gold NP with intermediate formation of polynuclear gold complexes. Both the chemical analysis data and the invariability of the height of the plasmon peak (see. Fig. 1) upon the change in the Au : rutin ratio from 12 : 1 to 1 : 1 indicates that neither the number nor the size of the NP formed are affected significantly by the rutin concentration in the system.

Consider the possible reasons and consequences of this unexpected finding. All of the bioflavonoids used have two hydroxy groups in the *ortho*-position of ring *B* and can be considered as derivatives of pyrocatechol, which is a two-electron reducing agent. It is known[35] that its analog, hydroquinone, reduces $Au^{III}$ to the metal even in cold solutions. According to potentiometric titration data,[36] $Au^{I}$ ion is formed as the first intermediate. This suggests that under the action of $Au^{III}$ the bioflavonoid molecule in

solution would be oxidized with transformation of the catechol ring *B* to the quinoid form, and hence complete reduction of $Au^{III}$ to the metal according to this reaction requires 1.5 equiv. of the bioflavonoid. Since an almost quantitative yield of $Au^0$ is attained for an Au : bioflavonoid ratio an order of magnitude lower than 1.5 : 1, for interpreting the experimental data, it is necessary to consider other $Au^{III}$ reduction reactions.

According to some published data, primary alcohols,[37–39] diols and polyols,[22–25] dextrin,[21] and cellulose can reduce $HAuCl_4$ to NP at elevated temperature.[22] This indicates that the disaccharide residue of rutin could be involved in the reduction of $HAuCl_4$. However, the approximately equal yields of gold NP of similar size irrespective of the excess of Au are observed also for quercetin and luteolin, *i.e.*, for bioflavonoids devoid of saccharide residues. In particular, in the case of luteolin, the yields of NP are equal for Au : bioflavonoid ratios of 1 : 1 and 15 : 1. Therefore, one must accept that $Au^{III}$ is reduced to the metal first of all through oxidation of substituted aromatic rings of the bioflavonoids. Reaction of this type is known for the enzyme quercetin 2,3-dioxygenase,[40] which catalyzes C—C bond cleavage of the pyrone ring *C* to give CO and oxidized product P.

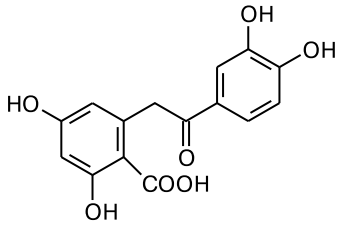


P

The final oxidant in this reaction is oxygen, which binds to the metal atom of the $Cu^{II}$ quercetin complex in the enzyme active site according to the peroxo type and subsequently oxidizes the quercetin ligand.[41]

Considering the stoichiometry of complete oxidation of bioflavonoids (for example, the oxidation of the luteolin molecule $C_{15}O_6H_{10}$ to $CO_2$ and $H_2O$ requires 29 oxidation equivalents [O]) shows that at a Au : bioflavonoid ratio of < 20 : 1, complete oxidation of the variable fraction of organic molecules can provide for the conversion of all $Au^{III}$ ions to $Au^0$. The non-consumed bioflavonoid molecules can remain in the initial form.

Thus, the presence of organic molecules in the system at relatively large excess of Au can in principle ensure the reduction of all Au ions. However, this brings about the question of why equal yields of $Au^0$ are formed despite considerably different reactant concentrations and chemically different reducing agents, although the intermediates and reactions involving them that occur during deep oxidation of bioflavonoids vary a lot. The simplest explanation is to assume the formation of a primary strong oxidant in the $H_2O$—$HAuCl_4$—bioflavonoid system, which can oxidize the organic molecules through subsequent reactions. This is based on the fact that the standard electrode potentials, $Au^+/Au$ of 1.85 V (see Ref. 42) and $Au^{3+}/Au$ of 1.627 V (see Ref. 43), are rather high. Therefore, the oxidizing ability of gold ions suffices for the oxidation of water not only to oxygen

$$O_2 + 4\,H^+ + 4\,e = 2\,H_2O$$

(the standard redox potential is 1.28)[44] but also to hydrogen peroxide. Under the experimental conditions, the proton concentration is $2.5 \cdot 10^{-4}$ mol $L^{-1}$. Thus it follows that the redox potential of water oxidation to hydrogen peroxide

$$H_2O_2 + 2\,H^+ + 2\,e = 2\,H_2O$$

in view of the standard value of 1.78 (see Ref. 44) is equal to 1.55 V. This conclusion is supported by direct calculation of the change in the standard free energy $\Delta G_{298}$ upon the reactions

$$4\,AuCl_4^-\,(H_2O\ solv) + 6\,H_2O\,(l) = 4\,Au\,(s) + 3\,O_2\,(g) + 12\,HCl\,(H_2O\ solv) + 4\,Cl^-\,(H_2O\ solv), \quad (1)$$

$$2\,AuCl_4^-\,(H_2O\ solv) + 6\,H_2O\,(l) = 2\,Au\,(s) + 3\,H_2O_2\,(H_2O\ solv) + 6\,HCl\,(H_2O\ solv) + 2\,Cl^-\,(H_2O\ solv) \quad (2)$$

(l, s, and g are the liquid, solid, and gaseous state, respectively, solv is solution) taking into account thermodynamic data,[45] which gives −73.6 and −3.8 kcal $mol^{-1}$ for Eqs (1) and (2), respectively. Since in both reactions the number of species increases, they become more favorable at higher temperature. In view of these data, we carried out experiments on the detection of $H_2O_2$ after the formation of gold NP using two procedures: titration by $KMnO_4$ and KI in acid medium.[46]

The control experiments demonstrated inapplicability of the former procedure, as rutin is oxidized with $KMnO_4$ with consumption of 10 equiv. of $KMnO_4$ per rutin molecule. The accuracy of the KI procedure is much lower, because the amount of hydrogen peroxide was estimated by comparing the color of a starch solution in the sample studied with the color of samples with specified $H_2O_2$ concentration. The control experiments showed the absence of the reaction of rutin with KI. After the formation of gold NP, no $Au^{III}$ ions able to react with KI are present in the system (see Fig. 6). Under these conditions, the formation of $I_2$ indicates the presence of other oxidants. This procedure demonstrated the formation of an oxidant in an amount corresponding to from 0.05 to 0.4 equiv. of $H_2O_2$ per mole of Au. In view of the high value of the normal redox potential of 1,2-quinone (+0.78 V), one can

conclude that this amount contains a contribution caused by oxidation of iodide ions by 1,2-quinone derivatives known to form in the system. However, comparison of the data obtained at different Au : rutin ratios (1 : 1, 4 : 1, and 6 : 1) for constant [Au] indicates that the amount of the oxidant formed in the system only increases with a decrease in the rutin concentration, and at a 6 : 1 ratio it is twice as high as the rutin concentration. This explicitly attests to the formation of either free hydrogen peroxide or Au peroxo complexes (either individual or on the NP surface), which decompose on treatment with sulfuric acid under conditions of the analytical experiment to give $H_2O_2$. Then the increase in their yield following a decrease in the content of the substrate being oxidized, *i.e.*, rutin, is quite reasonable and expectable. Thus, direct experiments confirm that oxidizing species are formed in the system after exhaustion of the primary $Au^{III}$ oxidant; this is in a qualitative agreement with the features of the mechanism of gold NP formation.

The full mechanism of NP formation in the presence of bioflavonoids is complicated, and currently only some assumptions can be made. Most pronounced is the difference between the stabilities of the NP obtained with an excess and deficiency of rutin. Since the capability of NP for association depends on their charge[47–49] (although even charged NP can enlarge, despite the Coulomb repulsion[50]), first of all, it is necessary to consider how the composition of the system can affect the NP charge. When rutin is present in excess, it is less likely to be deeply oxidized than when present in deficient amount; in the latter case, these reactions occur necessarily. It is also probable that the sequence of intermediates of the deep oxidation of rutin includes organic acids with a chelate unit (see the above example). These acids in the dissociated form may act as NP stabilizers ensuring the formation of charged and, hence, more stable NP at Au : rutin > 1 : 1.

For elucidating the nature of the catalytic action of bioflavonoids in the formation of NP, quantum chemical modeling was performed. The calculations were carried out by the density functional theory using nonempirical PBE functional and extended basis set for the SBK pseudopotential. The computing was done by the PRIRODA program suite[51] at the Joint Supercomputer Center of the Russian Academy of Sciences. As we previously showed theoretically, in water, $Au^I$ forms binuclear 1 : 1 complexes with quercetin (QcH) $Au_2Qc_2(H_2O)_2$. The calculation shows that association of these complexes

$$2\ [Au_2Qc_2(H_2O)_2] \rightleftharpoons [Au_2Qc_2(H_2O)_2]_2 \qquad (3)$$

produces a tetranuclear complex (Fig. 7). Due to the aurophilic interaction between the gold atoms of binuclear fragments, all of the Au—ligand bonds are elongated by 0.02 Å. The energy release is 10.2 kcal mol$^{-1}$. If it is assumed, according to Trouton´s rule, that the translational entropy

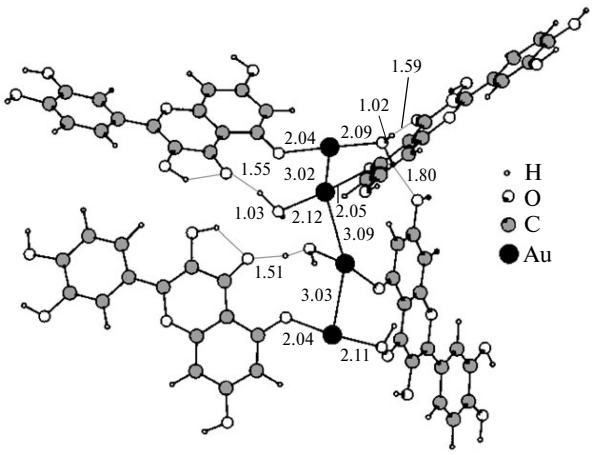


**Fig. 7.** Structure of the tetranuclear Au complex according to PBE DFT calculations. The bond lengths are in Å.

of vaporization of a solution is 21 cal mol$^{-1}$ deg$^{-1}$, then using the calculated statistical sums for the dimer and the tetramer in the ideal gas state, the equilibrium constant ($K$) of reaction (3) can be estimated as $10^4$. Thus, in the presence of quercetin (and, apparently, other bioflavonoids), the formation of chain of Au atoms able to act as NP nuclei is thermodynamically favorable. Meanwhile, at ~20 °C, when the NP formation in the Au—bioflavonoid system is substantially retarded, the flexibility of Au-chain nanostructures is very important. It allows their thermodynamically favorable transformation to ring structures. For this process with retention of the number of particles, the entropy changes little, and the equilibrium constant is an order of magnitude greater than $K$. This gives a nontrivial result, namely, the equilibrium number of short chains with dangling ends is relatively small and depends only slightly on the gold concentration in the system. This conclusion is in qualitative agreement with the observed regularities if one assumes that exactly the terminal gold atoms in the polynuclear chain-type gold complexes open for the reactions with the substrates are the catalytically active sites.

Meanwhile, the formation of polynuclear $Au^I$ complexes creates necessary conditions for realization of a high redox potential of these ions in chemical reactions, as only simultaneous reduction of several $Au^+$ ions to $Au^0$ may provide the multielectron oxidation of water molecules. As an example, we considered the addition of two coordinated water molecules in the binuclear complex $Au_2Qc_2(H_2O)_2$ at the Au—O bonds. This reaction gives binuclear HOAu—AuOH hydroxo complex containing two quercetin molecules as ligands and is accompanied by only a slight increase in energy (by 8.1 kcal mol$^{-1}$). This structure provides necessary conditions for the formation of both the $Au^0$—$Au^0$ fragment and hydrogen peroxide. Elucidation of the mechanism of water oxidation requires further experimental and theoretical studies.

Thus, relatively uniform and highly dispersed gold NP were obtained for the first time using the bioflavonoids rutin, quercetin, and luteolin as both the reducing agents and the stabilizers. A combination of the spectral method and atomic force microscopy was used to estimate the size and stability of the NP and to observe for the first time the topology of their surface. It was found that the NP size depends on the reducing agent concentration. In particular, at $[HAuCl_4] = 2.5 \cdot 10^{-4}$ mol $L^{-1}$, the decrease in the rutin concentration from $2.5 \cdot 10^{-4}$ to $5 \cdot 10^{-5}$ mol $L^{-1}$ increases the probability of formation of small-size gold NP and stabilizes the system. Note that during the formation of gold NP in the presence of rutin, free or bound $H_2O_2$ is produced. Theoretical analysis confirms the possibility of this process.

The development of new methods for NP preparation and their physicochemical investigation would provide a better understanding of the nature of nanosized effects and ordering of supramolecular structures and would extend the scope of applicability of gold NP in medicine, pharmacology, biology, and chemistry. A promising trend is studying the catalytic properties of the obtained systems in alkane oxidation reactions under mild conditions.

The authors are grateful to A. V. Ivanov (Institute of Problems of Chemical Physics, Russian Academy of Sciences) for quantification of gold in the samples.

This work was supported by the Division of Chemistry and Materials Science of the Russian Academy of Sciences (Program No. 1 "Theoretical and Experimental Study of the Nature of Chemical Bond and Mechanisms of Important Chemical Reactions and Processes").

## References

1. M. C. Daniel, D. Astruc, *Chem. Rev.*, 2004, **104**, 293.
2. P. Bishop, *Modern Supramolecular Gold Chemistry: Gold-Metal Interactions and Applications*, Ed. A. Laguna, John Wiley and Sons, Zaragoza, Spain, 2008, 525 pp.
3. J. Zhou, J. Ralston, R. Sedev, D. Beattie, *J. Colloid Interface Sci.*, 2009, **331**, 251.
4. A. N. Shipway, E. Katz, I. Willner, *Chemphyschem*, 2000, **1**, 18.
5. G. Han, P. Ghosh, V. M. Rotello, *Nanomedicine*, 2007, **2**, 113.
6. A. S. K. Hashmi, G. J. Hutchings, *Angew. Chem., Int. Ed.*, 2006, **45**, 7896.
7. M. Turner, V. B. Golovko, O. P. H. Vaughan, P. Abdulkin, A. Berenguer-Murcia, M. S. Tikhov, B. F. G. Johnson, R. M. Lambert, *Nature*, 2008, **454**, 981.
8. E. Quinet, L. Piccolo, F. Morfin, P. Avenier, F. Diehl, V. Caps, J. L. Rousset, *J. Catal.*, 2009, **268**, 384.
9. B. J. Jordan, R. Hong, G. Han, S. Rana, V. M. Rotello, *Nanotechnology*, 2009, **20**, 434004.
10. M. Haruta, *Nature*, 2005, **437**, 1098.
11. M. D. Hughes, Y. J. Xu, P. Jenkins, P. McMorn, P. Landon, D. I. Enache, A. F. Carley, G. A. Attard, G. J. Hutchings, F. King, E. H. Stitt, P. Jhonston, K. Griffin, C. J. Kiely, *Nature*, 2005, **437**, 1132.
12. R. M. Krieger, P. W. Jagodzinski, *J. Mol. Struct.*, 2008, **876**, 56.
13. X. H. Huang, I. H. El-Sayed, X. B. Yi, M. A. El-Sayed, *J. Photochem. Photobiology B — Biology*, 2005, **81**, 76.
14. G. Walther, L. Cervera-Gontard, U. J. Quaade, S. Horch, *Gold Bull.*, 2009, **42**, 13.
15. V. S. Kulikova, A. F. Shestakov, *Khim. Fizika*, 2007, **26**, 90 [Russ. J. Phys. Chem. (*Engl. Transl.*), 2007, **26**].
16. L. A. Levchenko, V. G. Kartsev, A. P. Sadkov, A. F. Shestakov, A. K. Shilova, A. E. Shilov, *Dokl. Akad. Nauk*, 2007, **412**, 500 [*Dokl. Chem.* (*Engl. Transl.*), 2007].
17. L. A. Levchenko, N. G. Lobanova, V. M. Martynenko, A. P. Sadkov, A. F. Shestakov, A. K. Shilova, A. E. Shilov, *Dokl. Akad. Nauk*, 2010, **430**, 773 [*Dokl. Chem.* (*Engl. Transl.*), 2010].
18. G. R. Xu, Y. Yuan, S. Kim, J. J. Lee, *Electroanalysis*, 2008, 1690.
19. B. Lim, P. H. C. Camargo, Y. N. Xia, *Langmuir*, 2008, **24**, 10437.
20. Z. G. Li, A. Friedrich, A. Taubert, *J. Mater. Chem.*, 2008, **18**, 1008.
21. H. Jang, Y. K. Kim, S. R. Ryoo, M. H. Kim, D. H. Min, *Chem. Commun.*, 2010, **46**, 583.
22. Y. P. Bi, G. X. Lu, *Mater. Lett.*, 2008, **62**, 2696.
23. S. E. Skrabalak, B. J. Wiley, M. Kim, E. V. Formo, Y. N. Xia, *Nano Lett.*, 2008, **8**, 2077.
24. T. Tang, I. W. Hamley, *Colloids and Surfaces A — Physicochemical and Engineering Aspects*, 2009, **336**, 1.
25. A. N. Grace, K. Pandian, *Colloids and Surfaces A — Physicochemical and Engineering Aspects*, 2006, **290**, 138.
26. Y. Shao, Y. D. Jin, S. J. Dong, *Chem. Commun.*, 2004, **9**, 1104.
27. L. Huang, Y. Zhang, Z. R. Guo, N. Gu, *Chin. Sci. Bull.*, 2009, **54**, 1626.
28. L. Barbu-Tudoran, G. Tomoaia, O. Horovitz, A. Mocanu, M. Tomoaia-Cotisel, *J. Optoelectronics Advanc. Mater.*, 2008, **10**, 2293.
29. M. A. Sirotkina, V. V. Elagin, M. V. Shirmanova, M. L. Bugrova, V. A. Kamensky, V. A. Nadtochenko, L. B. Snopova, E. V. Zagaynova, N. N. Denisov, *J. Biophotonics 3*, 2010, **10—11**, 718.
30. J. P. Cornard, J. C. Merlin, *J. Inorg. Biochem.*, 2002, **92**, 19.
31. Ch. E. Lekka, J. R. Sh. Meng, E. Kaxiras, *J. Phys. Chem. B*, 2009, **113**, 6478.
32. Z. Jurasekova, A. Torreggiani, M. Tamba, *J. Mol. Struct.*, 2009, **918**, 129.
33. R. Zigmondi, *Kolloidnaya Khimiya* [*Colloid Chemistry*] Unisa, Kiev, 1931, 325 pp. (in Russian).
34. N. G. Khlebtsov, *Anal. Chem.*, 2008, **80**, 6845.
35. P. E. Beamish, J. J. Russel, J. Seath, *Ind. Eng. Chem., Anal. Ed.*, 1937, **9**, 174.
36. N. K. Pshenitsyn, S. I. Ginzburg, I. V. Prokof´eva, *Zh. Analit. Khim.*, 1962, **17**, 343 [*J. Anal. Chem. USSR* (*Engl. Transl.*), 1962, **17**].
37. Y. J. Xiong, I. Washio, J. Y. Chen, H. G. Cai, Z. Y. Li, Y. N. Xia, *Langmuir*, 2006, **22**, 8563.
38. K. Kim, S. Choi, J. Cha, S. Yeon, H. Lee, *J. Mater. Chem.*, 2006, **16**, 1315.
39. Z. L. Jiang, Z. W. Feng, X. C. Shen, *Chin. Chem. Lett.*, 2001, **12**, 551.

40. R. A. Steiner, I. M. Kooter, B. W. Dijkstra, *Biochemistry*, 2002, **41**, 7955.
41. P. E. M. Siegbahn, *Inorg. Chem*., 2004, **43**, 5944.
42. A. M. Erenburg, B. I. Peshevitskii, *Zh. Neorgan. Khim.*, 1969, **14**, 2714 [*J. Inorg. Chem. USSR* (*Engl. Transl.*), 1963, **14**].
43. Yu. I. Usatenko, F. M. Tulyupa, Z. F. Garus, *Zh. Neorgan. Khim.*, 1968, **13**, 1083 [*J. Inorg. Chem. USSR* (*Engl. Transl.*), 1968, **13**].
44. *Spravochnik khimika* [*Chemist Handbook*], issue 2, *Khimiya*, Moscow, 1964, **3**, 1005 pp. (in Russian).
45. *Database of ther Department of Chemistry, Moscow State University, Termicheskie konstanty veshchestv* (*Thermal Characteristics of Substances*); http://www.chem.msu.su/cgi-bin/tkv.pl
46. S. A. Shapiro, M. A. Shapiro, *Analiticheskaya khimiya* (*Analytical Chemistry*), Vysshaya shkola, Moscow, 1963, 283 pp. (in Russian).
47. T. Laaksonen, P. Ahonen, C. Johans, K. Kontturi, *Chemphyschem*, 2006, **7**, 2143.
48. W. L. Huang, C. H. Chen, M. H. Huang, *J. Phys. Chem. C*, 2007, **111**, 2533.
49. T. Kim, C. H. Lee, S. W. Joo, K. Lee, *J. Colloid Interface Sci*., 2008, **318**, 238.
50. J. Wu, H. Zhang, J. H. Zhang, T. J. Yao, H. Z. Sun, B. Yang, *Colloids and Surfaces A — Physicochemical and Engineering Aspects*, 2009, **348**, 240.
51. D. N. Laikov, *Chem. Phys. Lett*., 2005, **416**, 116.

*Received April 12, 2010;*
*in revised form February 10, 2011*